FATIGUE CRACK GROWTH IN DOUBLE EDGE NOTCH TENSION SPECIMENS UNDER ELASTIC/PLASTIC LOADING

*G Green and **N Trigwell

SYNOPSIS

The possibility of thermal cycling producing strains exceeding yield in a welded configuration corresponding to a double edge notched tension specimen, prompted an investigation of fatigue crack growth under elastic/plastic loading conditions. It was decided to use a ΔJ approach similar to that proposed by Dowling and Begley.

A J Integral estimation procedure was employed to derive ΔK values from the area under the hysteresis loop. A computer was used to control this area to produce a constant ΔJ value and enable crack growth measurements to be made over a significant number of cycles.

Fractographic analysis of the specimens indicated that crack growth occurred by fatigue throughout the stress range studied. No evidence of ductile tearing appeared in the fracture surface. The relationship between ΔK and da/dn remained sensibly linear from the linear elastic through to the fully plastic range and a crack growth law was derived, which is similar to that found by other workers. Significantly, this law predicts faster growth rates than those assumed using an upper bound crack growth rate based on linear elastic tests.

INTRODUCTION

A service problem involving a component subjected to periodic exposure to a thermal stress, which could produce strains in excess of yield, stimulated a study of fatigue crack growth under elastic/plastic loading conditions.

* CEGB SW Region, Scientific Services Department, Bristol UK
** Testwell Ltd, Daventry, UK

The component configuration approximated to a double edge notch tension specimen and this geometry was chosen to model fatigue crack growth and to obtain data for use in a fracture mechanics assessment of the component. This paper describes the use of a J integral approach to characterise fatigue crack growth in double edge notch tensile specimens subjected to elastic/plastic loading.

THE J INTEGRAL APPROACH

Dowling and Begley (1) defined the J integral for the characterisation of fatigue crack growth as being proportional to the area under the load displacement hysteresis loop for which the crack is open. For bend geometries there is a constant relationship between the J integral and the area under a load displacement curve from elastic through to elastic/ plastic behaviour. However, for tension geometries this relationship differs between the elastic and the elastic/plastic regions of deformation. It is possible to estimate the J integral for any geometry by defining (following Sumpter and Turner (2)).

$$J = \frac{\eta U}{B(W-a)} \qquad (1)$$

and splitting the load deflection curve into an elastic and plastic part (Ue and Up).

The J integral is now defined as:

$$J = \frac{\eta e\ Ue}{B(W-a)} + \frac{\eta p\ Up}{B(W-a)} \qquad (2)$$

ηe is defined as $\frac{2(W-a)}{P_L}\ \frac{Y^2}{Z}$

and ηp is defined as $-\frac{(W-a)}{W}\ dP_L/da$

The value of ηe is gauge length dependent, due to the contribution of elastic deflections remote from the crack. In these experiments a gauge length of 125mm was chosen for displacement measurements as this gave values of ηe and ηP which were similar over the crack growth range of interest. The ηe values are calculated from the elastic compliance function of Tada et al (3) and ηP values from the limit load, P_L (4)

$$P_L = \left[\ 1 + \ln \frac{(1 - a/2W)}{(1 - a/W)}\ \right] 1.55\ \sigma y\ (W-a) \qquad (3)$$

The ηe and ηp values used in the investigation are given in Table 1. Note that as the crack length increases ηe approaches ηp, making J evaluation less sensitive to methods of partitioning elastic and plastic energy terms.

Table 1 ηe and ηp Values used to evaluate J

a/w	ηe	ηp
0.3	1.31	0.51
0.4	0.62	0.52
0.5	0.60	0.53
0.6	0.57	0.54
0.7	0.51	0.57

EXPERIMENTAL PROCEDURE

The component configuration consisted of a weld between two Carbon Manganese steels EN3A and BS 1501, 28A. The weld metal was a low carbon steel deposited using a manual metal arc process. Test specimens were manufactured such that the following specimens were available; those in which crack growth occurred wholly within the weld metal, those in which crack growth occurred in the heat affected zone of the EN 3A steel and finally those in which crack growth occurred in the heat affected zone of the BS 1501 28A steel.

The specimen dimensions were as follows; W = 100mm, B = 10mm, total initial crack length 42mm. The specimens contained spark eroded starter notches and fatigue precracks were grown from these under elastic loading conditions.

Tests were performed in a 400kN Losenhausen UHS40 testing machine modified for servo-hydraulic operation. An LVDT transducer was mounted each side of the specimen on the 125mm gauge length and their outputs were averaged via an (A + B)/2 unit to help reduce the effect of any bend in the specimens upon displacement measurements.

Elastic and plastic strain energy inputs to the specimen (ΔU_E and Δ Up) were computed from load-displacement measurements on the specimen. The cyclic displacement was controlled to maintain the combined value of these strain energies (ΔU_{Total}) at a constant level. Fatigue crack propagation was monitored optically to enable calculation of $\frac{da}{dN}$ versus ΔJ relationsips.

Crack growth rates were averaged between the two cracks in the specimen

A 12 bit Digital to Analogue converter and a 10 bit twin channel tracking type analogue to digital converter were used to interface the testing machine/specimen to a Commodore CMD 3032 Mini computer. The ADC channels were calibrated to monitor load and displacement. The DAC was used to produce the cyclic command waveform. The testing machine was operated under displacement control.

A computer programme was developed to log load and displacement around a complete cycle. Any crack closure "tail" on the strain hysteresis curve was then removed. In practice crack closure tails on the strain hysteresis loops proved to be very small. The total strain energy input ΔU_T to the specimen was then calculated and the demand signal was adjusted to maintain this at a constant level. The procedure was performed typically every 10 cycles depending upon the rate of crack advance. The cyclic wave form used was triangular to facilitate easier computation of the necessary changes of displacement level to maintain the constant value of ΔU_T. The frequency used was 0.1Hz.

Estimates of fatigue growth rates under LEFM conditions were obtained on three specimens. Fatigue crack propagation was then performed under displacement control at four or five values of ΔU_T. (The value of ΔU_T was always increased in level through a test, never decreased).

Upon completion of the tests each specimen was broken open in liquid nitrogen. One fracture surface of each crack was mounted for examination in a scanning electron microscope. The matching fracture face was Nickel plated, sectioned and prepared for metallographic examination.

Three specimens were tested with the following identities and initial fatigue crack locations.

Specimen 3 with cracks in the weld metal.
Specimen 4 with cracks in the Heat affected zone of EN3A.
Specimen 5 with cracks in the Heat affected zone of BS 1506.

RESULTS

Typical strain hysteresis loops for specimen 4 are shown in Figure 1. Note that large proportions of plastic displacements are only present in the final strain energy range, and also that there is little evidence of crack closure in the hysteresis loops. Crack growth versus cycles during two of the strain energy inputs are shown in Figure 2. Note the good linear relationship confirming a constant crack growth rate. Crack growth data obtained on each specimen are given in Table 2. These data are shown in Figure 3. The data are plotted as a function of ΔK or $\surd E^1 \Delta J$, where data were obtained under elastic/plastic conditions.

The data from each specimen were analysed in the form of a Paris relationship:

$$\frac{da}{dN} = C\Delta K^m$$

and the indices and constants for each data set and the pooled data sets are given in Table 2.

In most cases crack growth occurred within the crack plane, but one crack tip in specimens 5 and 4 developed extensive shear lips and showed surface growth at approximately 45^o to the initial crack plane. However, in plane growth occured within the central portion of the specimen.

Fractographic examination of the specimens indicated some microvoids associated with the fatigue crack growth even at low ΔJ values. There were also signs of damage on the fracture surfaces due to crack closure. These signs were particularly obvious on regions which had experienced crack growth at high ΔJ. The damage due to crack closure could have masked the presence of microvoid coalescence at high ΔJ vaues. However, comparison of the fatigue fracture faces with ductile fractures produced in the parent plates did not reveal similar void sizes or depths.

Metallographic examination indicated that the cracks did not deviate significantly from the microstructure in which they were grown initially. There was a tendency for cracks in the heat affected zones to grow towards the parent plate, but not into the weld metal.

DISCUSSION

The extremely good linearity displayed by the crack growth plots at constant strain energy inputs confirms that this parameter characterises crack growth. The linear relationships between ΔK or $\surd E^1 \Delta J$ and crack growth rate also indicates the effectiveness of the cyclic J integral in characterising crack extension from the elastic into the elastic/plastic range.

The crack growth laws derived indicate an exponent greater than the value of 3, which is suggested in an upper bound to the fatigue crack growth law for carbon manganese steels (Lindley and Richards (5)).

Sensitivities to ΔK in excess of ΔK^3 have been reported by other workers, Priddle (6), Musava and Radon (7) and Pook (8). These data include those in which loading conditions are entirely elastic and those in the elastic/plastic region and in which the crack growth mechanism was by fatigue. Note that in the tests reported here crack growth was essentially by fatigue with no evidence of ductile tearing.

It is possible that accelerations in crack growth rates could be caused by experimental and analytical factors such as over estimates of crack length and incorrect estimates of the J integral. Surface crack lengths did not exceed interior crack length measurments. In many cases there was a minor amount of

crack tunnelling. the estimated J integral could differ from the true appliedΔK at the crack tip, due to problems of interpreting crack closure in the hysteresis loop. In these experiments only small amounts of crack closure were detected in the hysteresis loops, although, evidence of crack closure was observed. This discrepancy is no doubt due to insensitivity caused by the transducer location remote from the crack tip region. The estimated J values therefore if anything overestimate the ΔK values. Finally, there is a possible problem with the method of estimating J from the partitioning of the hysteresis loop into elastic and plastic parts. Such problems become significant only in the cases where the elastic and plastic areas are comparable in magnitude. If the η values are too dissimilar an incorrect estimate of J will result. In these experiments the plastic displacements were significant in the final high ΔJ tests for which the crack length ratio was in excess of a/W 0.5. Consideration of the η factors in Table 1 indicates a maximum error of 15% in J, if all the energy were assumed to be plastic (for a/W = 0.5). This would correspond to an increase in exponent in the crack growth law to 3.05 from 3. Errors in J are much smaller than this value. Clearly, the values of 3.21 for the exponent derived from this study cannot be attributed to any of these experimental and analytical problems. The crack growth law is in excess of the upper bound value of 3 suggested by Lindley and Richards (5).

Fractography indicated some evidence of voids in the fracture surface, although there was no evidence of ductile tearing. The presence of voids is to be expected since these will nucleate and grow in the strain field at the crack tip. The size and number of voids on the fracture surface are expected to increase with increasing plastic strain with increasing ΔJ. It has been noted that the void size and topography did not appear similar to that obtained in monotonic ductile fracture of the plate material. This is because of the lower strain levels experienced in the fatigue tests than in the monotonic fracture test and also perhaps due to differences in strain hardening in the crack tip region in fatigue compared with monotonic fracture. The absence of ductile tearing in these experiments is also supported by the final ΔJ values, 100 Nmm^{-1} for the weldment and 70 Nmm^{-1} for the plate materials. These are less than reported values for MMA welds of approximately 200 Nmm^{-1} (Gates et al (9)) in thicker sections and those for similar plate in 25mm sections ~100 Nmm^{-1} Green (10). In the absence of specific fracture toughness values, these reported estimates can only be taken as an approximate guide to the material toughnesses, but it should be remembered that thinner sections can display significantly greater toughnesses than thicker sections, Krafft et al (11). The maximum ΔJ values experienced in these tests are unlikely to be equal to the fracture toughness of the material.

The experiments reported here indicate that the interpretation of the J integral as used by Dowling and Begley (1) and Dowling (12) which was demonstrated to characterise fatigue crack growth under elastic and elastic/plastic loading in Compact Tension specimens and Centre Cracked Plates, can be used to characterise fatigue crack growth in other geometries, providing that monotonic fracture is avoided.

CONCLUSIONS

A cyclic J integral approach has been used to determine fatigue crack growth rates in double edge notch tension specimens from elastic through to elastic/plastic loading conditions.

Crack growth laws remained similar throughout this loading range and were identical to those obtained in carbon manganese steels by other workers.

Crack growth was by a fatigue mechanism throughout, with no evidence of ductile tearing. The observed increase in exponent in the crack growth rate law above the previously proposed upper bound of 3 is not due to contributions from monotonic fracture.

The cyclic J integral may be able to characterise fatigue crack growth under elastic plastic conditions through a range of geometries.

ACKNOWLEDGEMENTS

This paper is published with the permission of the Director General of the CEGB, SW Region, Bristol, Great Britain.

MET03GGVHOSP
GEMINI DISK WENDY

SYMBOLS

a = crack length
B = specimen thickness
C = Constant in crack growth rate equation
$\frac{da}{dN}$ = Crack growth rate per cycle
ΔJ = Cyclic J integral
ΔK = Alternating Stress Integrity
E^1 = Young's modulus in plane strain
J = J Integral
m = exponent in crack growth rate equation
P_L = Limit load
U = Area under load displacement record
Ue = Elastic area of load displacement record
Up = Elastic area of load displacement record
W = Specimen width
Y = Stress Intensity Correction factor
Z = Compliance function including uncracked specimen deflections.
η = Geometry dependent factor relating J to U
ηe = Geometry dependent factor relating elastic J to elastic U
ηp = Geometry dependent factor relating plastic J to plastic U
σ = Yield stress

REFERENCES

1. Dowling N E and Begley J A, ASTM STP 590, 1976, pp 83-104.
2. Sumpter J D G and Turner C E, ASTM STP 601, 1976, pp 3-18.
3. Tada H et al, 1973, 'The Stress Analysis of Cracks Handbook'. Del Research Corporation.
4. Ewing D J F and Hill R, 1967, J Mech. Phys, Solids, Vol 15, p 115.
5. Lindley T C and Richards C E, 1972, Engn. Fract. Mechs., Volume 4, p 951
6. Priddle E K, Int Jnl. Pres. Vess. and Piping, Vol 4, No 2, April 1976, pp 89-117.
7. Musava J K and Radon J C, 1980, Proc. 3rd Coll. on Fracture and Fatigue, ed J C Radon, London Sept. 1980.
8. Frost N E, Pook L P and Denton K, Eng. Fract. Mech. Vol 3, 1971, p 109.
9. Gates R S et al, 1983, CEGB SW Region, Unpublished work.
10. Green G, 1982, Paper presented at ECF4, Leoben, Austria.
11. Krafft J M et al, 1961, Proc Symp. Crack Propagation, Cranfield, p8.
12. Dowling, N E, 1976, ASTM STP 601, pp 19-32.

TABLE 2

FATIGUE CRACK GROWTH RATE DATA

SPECIMEN NUMBER	ΔK MPa $\sqrt{m}$	ΔJ Nmm^{-1}	da/dN mm/cycle
3	16.90	-	4.54×10^{-5}
	20.04	-	5.98×10^{-5}
	21.45	-	6.50×10^{-5}
	87.7	33.5	5.86×10^{-3}
	105.9	48.5	11.71×10^{-3}
	134.3	78.1	14.60×10^{-3}
	152.1	100.0	20.98×10^{-3}
	$da/dN = 9.41 \times 10^{-9} \Delta K^{2.95}$		
4	19.9	-	4.60×10^{-5}
	44.19	8.45	9.94×10^{-4}
	63.9	17.70	3.60×10^{-3}
	88.7	34.08	4.53×10^{-3}
	110.0	52.40	1.45×10^{-2}
	132.8	76.40	3.72×10^{-2}
	$da/dN = 2.47 \times 10^{-9} \Delta K^{3.34}$		
5	19.5	-	2.78×10^{-5}
	46.3	9.27	1.65×10^{-3}
	71.6	22.20	2.76×10^{-2}
	107.5	50.10	1.46×10^{-2}
	126.2	69.00	3.70×10^{-2}
	$da/dN = 6.83 \times 10^{-10} \Delta K^{3.65}$		
	All data		
	$da/dN = 3.9 \times 10^{-9} \Delta K^{3.21}$		

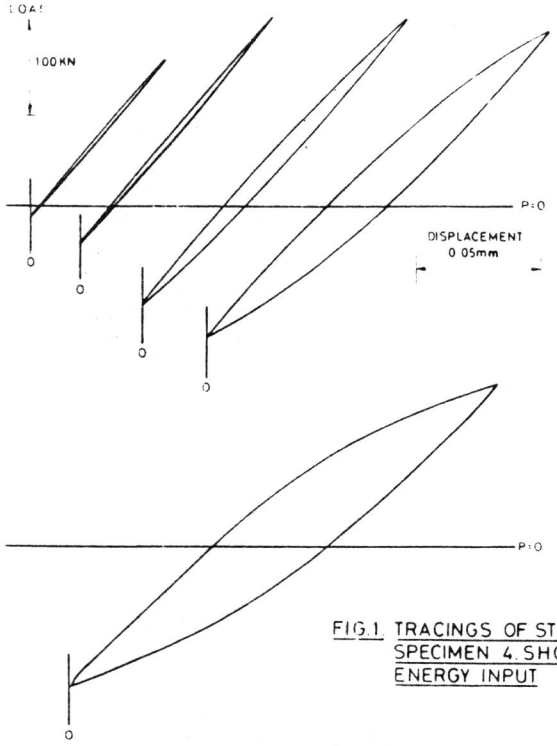

FIG.1. TRACINGS OF STRAIN HYSTERESIS LOOPS FOR SPECIMEN 4 SHOWING VARIATION IN STRAIN ENERGY INPUT

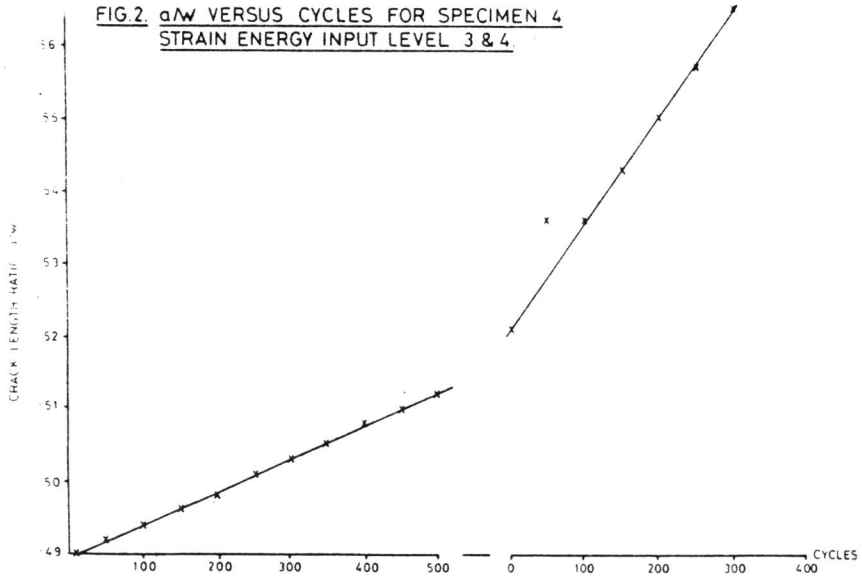

FIG.2. a/w VERSUS CYCLES FOR SPECIMEN 4 STRAIN ENERGY INPUT LEVEL 3 & 4.

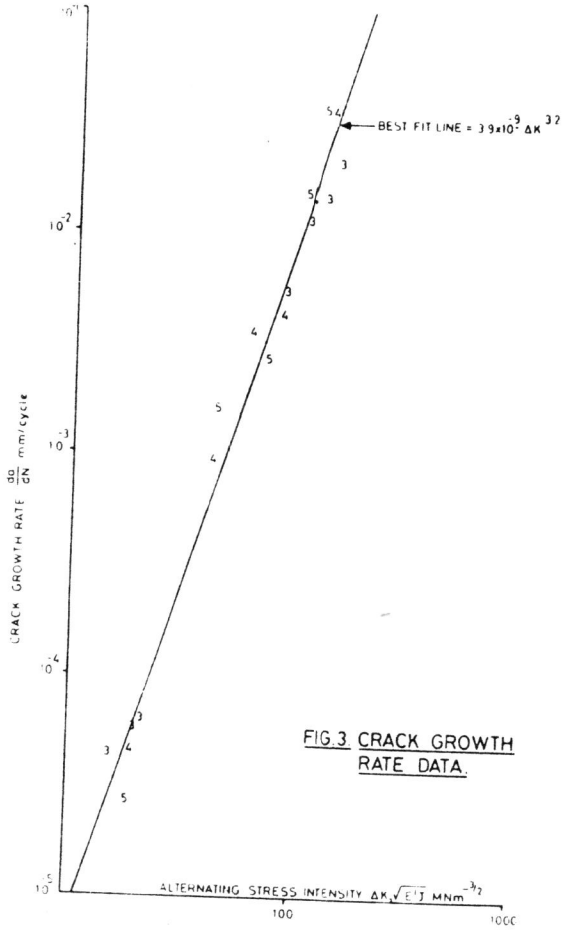

FIG.3. CRACK GROWTH RATE DATA.